iJRASET
International Journal For Research in
Applied Science and Engineering Technology

INTERNATIONAL JOURNAL FOR RESEARCH

IN APPLIED SCIENCE & ENGINEERING TECHNOLOGY

Volume: 14 **Issue:** VIII **Month of publication:** August 2026

DOI: https://doi.org/10.22214/ijraset.2026.84516

International Journal for Research in Applied Science & Engineering Technology (IJRASET)
ISSN: 2321-9653; IC Value: 45.98; SJ Impact Factor: 7.538
Volume 14 Issue VII July 2026- Available at www.ijraset.com

Swift Synthesis of Nickel Nanoparticles and their Antibacterial Studies through Green and Sustainable Method Using Terminalia Mantaly Leaf Extract

Bandari Lavanya[1], Y. Aparna[2]
[1, 2]*Department of Physics, Jawaharlal Nehru Technological University Hyderabad, Telangana 50085, India*
[1]*Department of Physics, Anurag University, Hyderabad, Telangana 50088, India*

Abstract: In this paper, we report a swift and simple green synthesis method to produce nickel oxide nanoparticles (NiO NPs) utilizing, for the first time, Terminalia mantaly leaf extract to improve their properties. Fourier transform infrared spectroscopy (FTIR), X-ray diffraction (XRD), scanning electron microscopy (SEM), energy-dispersive X-ray spectroscopy (EDAX), and photoluminescence studies were carried out on the synthesised samples. Antibacterial studies were performed, and results are presented in this paper. The results confirm that Terminalia mantaly biomolecules induce the reduction of nickel ions to NiO NPs and function as a capping and stabilising agent, enhancing biological performance.

I. INTRODUCTION

Nanoparticles have gained significant importance in both biological and non-biological fields because of their exceptional physico-chemical characteristics. Their distinctive features, including morphology, particle size, shape, crystalline structure, high surface-area-to-volume ratio, and unique optical, magnetic, chemical, and mechanical properties, make them suitable for a wide range of applications. Conventional methods for nanoparticle synthesis, such as hydrothermal processing, microemulsion techniques, electrospraying, co-precipitation, laser ablation, and sol–gel methods, have been widely employed. However, these techniques often require costly equipment, produce relatively low yields, and rely on hazardous chemicals that may adversely affect the environment.

To overcome these limitations, increasing attention has been directed toward green synthesis approaches that utilize plant extracts, microorganisms, and enzymes as eco-friendly alternatives. This sustainable strategy has become increasingly popular because it is economical, rapid, environmentally benign, and suitable for large-scale production. In plant-mediated synthesis, phytochemicals present in the extracts function as both reducing and stabilizing agents by interacting with metal ions and facilitating nanoparticle formation. Additionally, the natural microstructure of plant tissues, including leaves and petals, can serve as biological templates that regulate nanoparticle growth, control particle size, and minimize aggregation, resulting in the formation of stable nanoparticles.

Nickel oxide (NiO) is an inorganic black crystalline substance with a band gap ranging from 3.6 eV to 4.0 eV. It exhibits excellent electrochemical performance and also possesses magnetic, mechanical, electronic, and optical properties [11,14]. Nickel oxide (NiO) is an important transition metal oxide that has gained increasing attention due to its potential use in various applications [16]. Nickel-based nanoparticles, particularly metallic nickel (Ni^0), have attracted considerable interest because of their broad range of industrial and technological applications. In addition, they are promising electrode materials for supercapacitors due to their excellent electrochemical performance. Their unique surface characteristics improve the interaction between active materials and conductive carbon supports, thereby preventing the loss of catalytic components through detachment or desorption. This enhanced interfacial contact facilitates efficient electron transport and increases the overall electrical conductivity of the system NiO nanoparticles have demonstrated significant potential in antifungal, antibacterial, antioxidant, anti-inflammatory, anticancer, and enzyme inhibition activities [7]. Nickel oxide nanoparticles (NiO NPs) can be obtained through a simple and practical method by heating nickel(II)-based compounds such as hydroxides, nitrates, and carbonates [12].

Further nickel oxide nanoparticles (NiO NPs) have received increasing scientific attention because of their outstanding physicochemical and electrochemical characteristics. These include excellent chemical stability, high coercivity, significant magnetocrystalline anisotropy, large specific capacitance, superior durability, electrochemical stability, and intrinsic antiferromagnetic behaviour.

Owing to these properties, NiO nanoparticles have found widespread applications in catalysis, biomedical technologies, supercapacitor fabrication, and dye-sensitised solar cells. In addition, they possess diverse biological activities, including antioxidant, antimicrobial, antifungal, anticancer, cytotoxic, enzyme inhibitory, and environmental remediation capabilities, making them suitable for numerous catalytic and biomedical applications. Their high surface area, ability to adsorb and release metal ions, and controlled cytotoxic effects further support their potential use in therapeutic and drug-delivery systems.

Various physical and chemical techniques have been developed for the preparation of NiO nanoparticles, including sol–gel processing, spray pyrolysis, electrodeposition, chemical bath deposition, and spin coating. Although these methods can produce high-quality NiO thin films, they often involve complex procedures, high energy consumption, and limited control over particle morphology. In particular, synthesising highly porous NiO nanoparticles with particle sizes below 20 nm remains challenging, and the resulting materials frequently exhibit poor adhesion and inadequate cycling stability. Consequently, environmentally sustainable synthesis strategies have emerged as promising alternatives. Green synthesis approaches offer several advantages over conventional methods, including reduced energy requirements, minimal generation of hazardous waste, improved environmental compatibility, and simplified processing.

Terminalia mantaly has attracted research interest because of its Antitumor, antidiabetic, and antihypertensive drug properties [22]. Terminalia mantaly is a deciduous tree belonging to the family Combretaceae. Many scientific studies have examined the antibacterial, antiprotozoal, antidiarrheal, anti-inflammatory, anti-tumour, and wound-healing properties of this tree [23]. The present study explores the fabrication of NiO nanoparticles employing Terminalia mantaly leaves as natural reducing and stabilising agents. This plant-assisted synthesis route offers several benefits, including high product yield, rapid reaction time, operational simplicity, economic feasibility, and environmental sustainability. In continuation of our earlier work on the green synthesis of metal nanoparticles using Terminalia mantaly leaf extracts [1, 19, 20, 21], we have studied the synthesis of NiO nanoparticles, and the results are reported in this paper, including characterisation and antibacterial studies.

II. MATERIALS AND METHODS

A. Materials

Zinc Nitrate hexahydrate (Analar grade) was obtained from Sigma-Aldrich. Healthy Terminalia mantaly Leaves were collected from Terminalia mantaly trees in the area of Venkatapur Village. These were identified by the Department of Botany, Kakatiya University, Warangal.

B. Method for preparation of leaf extract

The collected leaves were washed with tap water for 15 minutes in order to make them dust-free. Further, they were washed thoroughly using double-distilled water to make them clean. These leaves were dried at room temperature, cut into small pieces by hand and then finely powdered using a kitchen grinder. The powder was sieved with a domestic polymer sieve in order to avoid metal contamination.

30 grams of leaf powder was weighed and added to 200 mL of water in a 500 mL beaker. The mixture was stirred for 60 minutes using a magnetic stirrer at 80 °C. The liquid was allowed to cool and filtered in a conical flask using Whatman 60 filter paper. The resultant plant extract was again filtered with Whatman 60 filter paper and was stored in a refrigerator in a tightly sealed glass bottle at 4°C for future use.

C. Synthesis of NiO nanoparticles

5 g of $Ni(NO_3)_2 \cdot 6H_2O$ precursor was added to 20 mL of plant extract and heated at 60 °C for 2 h on a magnetic stirrer, resulting in a fine paste. This was washed with distilled water and treated at 100°C for 1hour, then the resultant was transferred directly to another furnace, which was maintained at 400°C and calcined for 2 hours at the same temperature. The calcined product was then crushed into a fine powder by using a mortar and pestle. The obtained product was of greyish black colour and was stored in an airtight container until further use or analysis [23,24].

III. CHARACTERISATION TECHNIQUES

A. X-ray diffraction (XRD)

The X-ray diffraction pattern of synthesized NiO nanoparticles by using mantaly leaf extraction is shown in fig.1. The diffraction peaks of synthesised NiO particles using leaf extract of are obtained approximately at an angles 37.28547, 43.33088, 62.92415, 75.46974 and 79.45466, corresponding to (111), (200), (220), (311) and (222).

The pattern forms well-defined, sharp, intense peaks, confirming the formation of highly crystalline NiO NPs. The observed diffraction peaks are in good agreement with the JCPDS card No. 78-0643, indicating the successful formation of NiO NPs. Scherer's formula is used to calculate the particle size,

$$D = \frac{k\lambda}{\beta cos\theta} \quad ---------- (1)$$

Where D is crystallite size, k is a constant which is equal to 0.9, 2θ is the Bragg angle, β is the full-width at half maximum (FWHM) in radians, and λ is the wavelength of X-rays used, i.e. 1.54å. The formed nanoparticles are cubic, face-centred, with an average crystallite 25.27nm TM leaf extracts

By using Bragg's equation, the interplanar distance d is calculated. i.e.

$$n\lambda = 2d \sin\theta \quad ....(2)$$

As the synthesised NiO nanoparticles are found to have a face-centred cubic structure. Hence, the lattice parameter 'a' is calculated by using the formula

$$a = d(\sqrt{h^2} + k^2 + l^2) \quad .... (3)$$

The Microstrain of the nanoparticle is calculated by using the formula

$$\varepsilon = \frac{\beta}{4\ tan\theta} \quad ... (4)$$

It is observed that the micro strain value decreases with increasing angle θ value.

The length of dislocation lines per unit volume is defined as Dislocation density δ. From the XRD pattern, the dislocation density is also calculated by the equation

$$\delta = \frac{1}{D^2} \quad ... (5)$$

Where D is the crystalline size.

The interplanar distance, lattice parameter, particle size, and micro strain values are calculated and tabulated in Table 1.

Sample	Average d-spacing (nm)	Scherrer Crystallite Size (nm)	Lattice Parameter (Å)	Unit Cell Volume (Å³)	Dislocation Density ($\times10^{14}$ m^{-2})	Scherrer Microstrain
TM	0.1687	25.27	4.1732	72.67	16.94	0.00295

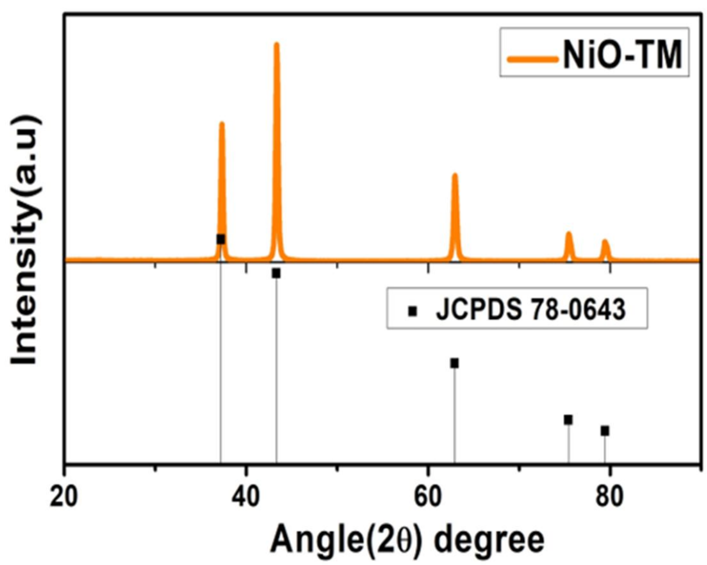

Figure 1. XRD pattern of NiO nanoparticles synthesised using *Terminalia mantaly* leaf extract.

B. Fourier Transform Infrared Spectroscopy (FTIR)

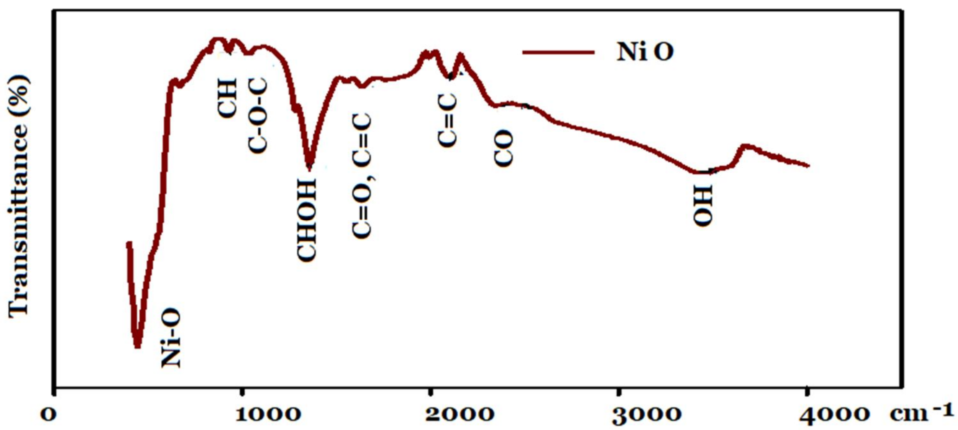

Figure 2. FTIR spectrum of green-synthesised NiO nanoparticles showing the characteristic Ni–O stretching vibration along with absorption bands.

Fig. 2 shows the FTIR spectrum of the synthesised NiO nanoparticles, which showed an absorption band at 454 cm^{-1}, which was attributed to the Ni–O stretching vibration in NiO, indicating the formation of nickel oxide. The broad band in the range 3417 cm^{-1} is attributed to OH stretching vibrations of hydroxyl groups and of adsorbed water. In the infrared spectra, peaks were observed at 1660 cm^{-1}, 1370 cm^{-1}, and 1034 cm^{-1}, corresponding to C=O stretching, C–H bending, and C–O stretching, respectively, suggesting the presence of phytochemicals obtained from the plant extract that behaved as reductants and stabilisers. The weak band at 912 cm^{-1} is attributed to C–H deformation and the weak band at 2118 cm^{-1} to C≡C stretching/combination bands, whereas the band at 2363 cm^{-1} is attributable to the CO_2 absorption by the atmosphere.

C. Field Emission Scanning Electron Microscope (FESEM)

Fig. 3(a) shows the FESEM image, which shows that NiO nanoparticles form dense clusters and are largely quasi-spherical to polyhedral in shape, with noticeable agglomeration, and are interconnected with each other, creating a porous network. The particles are evenly distributed but in a fused state, forming larger aggregates, with some rough surface grains, suggesting the presence of NiO crystalline grains. Faceted shape indicating good crystallinity, which is in agreement with the XRD studies. The average estimated size is 20-60 nm, while some aggregates are as large as 200 nm.

The morphology observed suggests that the green synthesis method has successfully synthesised nanostructured NiO having a high surface area. This plant extract provided some reducing and stabilizing action during the plant extract preparation and may have controlled nucleation and prevented a buildup of too large particles. These organic residues were removed during calcination; however, the free movement of the particles led to some sintering, causing clusters of nanoparticles to form.

D. EDX Analysis

The Energy Dispersive X-ray Spectroscopy (EDX) spectrum, shown in Fig. 3(b), confirmed the successful synthesis of NiO by showing two large peaks at the energies of Ni and O. The strong Ni peaks at ca 0.85 keV (Ni Lα) and 7.47 keV (Ni K_{α}) and the O peak at ca 0.52 keV are typical of NiO. No other metallic impurity peaks are notable in the spectrum, and it is clear that the synthesised nanoparticles are highly pure. The quantitative analysis also validates that nickel is the major elemental constituent with the expected amount of oxygen for the formation of NiO. Minor deviations from the ideal Ni:O stoichiometric ratio are possible due to the limited sampling depth of EDX, the presence of oxygen vacancies, surface adsorption of atmospheric species and instrument limitations.

Based on the EDX result and FESEM observation, the centralised high-purity NiO NPs, which are nanometer-sized, have been successfully synthesised.

International Journal for Research in Applied Science & Engineering Technology (IJRASET)
ISSN: 2321-9653; IC Value: 45.98; SJ Impact Factor: 7.538
Volume 14 Issue VII July 2026- Available at www.ijraset.com

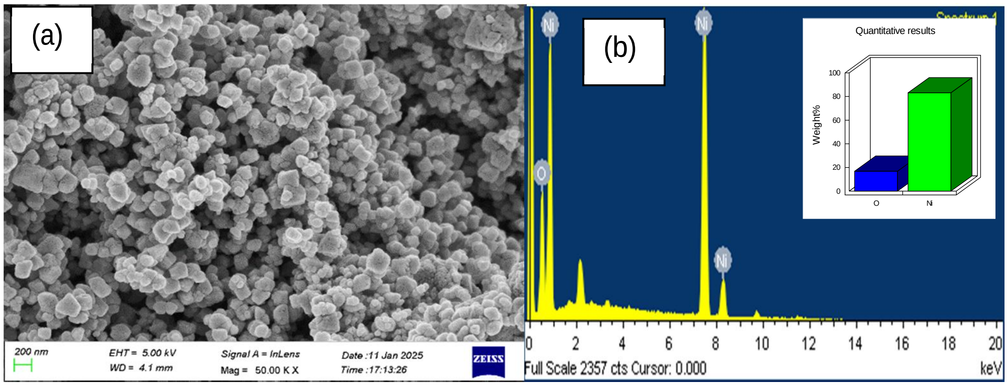

Figure 3. (a) FESEM micrograph showing the surface morphology of the green-synthesised NiO nanoparticles and (b) EDX spectrum confirming the elemental composition of nickel (Ni) and oxygen (O).

E. UV-VIS Spectroscopy

The UV–Visible spectroscopy of the synthesised NiO nanoparticles was examined in the range of wavelengths 200 – 600 nm, as illustrated in Fig. 4(a). The NiO intrinsic electronic transition from the valence band to the conduction band is shown by the absorption edge that occurs in this spectrum at around 328 nm. As a result of this absorption, we conclude the formation of NiO semiconductor nanoparticles and the ability to absorb photons in the UV region.

A charge-transfer transition O^{2-} (2p) → Ni^{2+} (3d) is responsible for the relatively intense absorption in the UV region that is intrinsic to NiO nanoparticles. At wavelengths beyond 350 nm, a gradual decrease in absorbance shows that absorbance decreases within the visible range. This slight broadening of the absorption edge can be attributed to the nanoscale size of the particles, structural defects, surface states and oxygen vacancies from the green synthesis process. Phytochemicals of the leaf extract of Terminalia mantaly as a capping agent can also impart the optical absorption effect by altering the property of the nanoparticle surface.The Tauc relation was used for the determination of the optical band gap:

$$(\alpha h\nu)^2 = A\,(h\nu - E_g)$$

Here α is the absorption coefficient, hν is the photon energy, A is a proportionality constant, and Eg is the optical band gap. The exponent n=2 was assumed for NiO, since it is considered a direct band gap semiconductor and a graph of $(\alpha h\nu)^2$ as a function of photon energy (hν) was plotted, as seen in Fig. 4(b).

The extrapolated linear part of the Tauc plot, onto the energy axis, gave the optical band gap at 3.24 eV. The value is in good agreement with the reported value for the band gap in NC NiO (3.2–3.8 eV) and is slightly higher than the value of NiO bulk material, which is generally believed to be related to the particle size being nanocrystalline. This can be understood by various reasons such as improved crystallinity, lattice strain, oxygen vacancies, surface defects, and the role of phytochemical capping molecules in green synthesis. The relatively broad band gap revealed the potential of prepared NiO-based nanoparticles for good optical transparency in the visible region with high absorption in the UV region. These optical properties are ideal for photocatalysis and antibacterial applications.

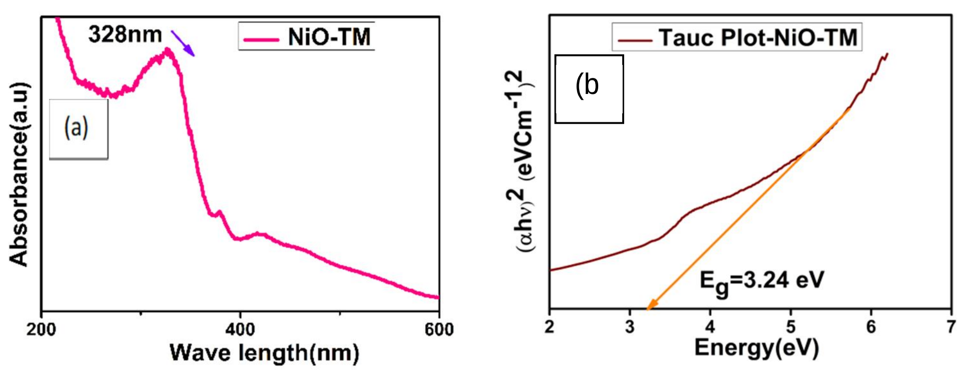

Figure 4. (a) UV–Visible absorbance spectrum of NiO nanoparticles synthesized using *Terminalia mantaly* leaf extract and (b) Tauc plot showing the estimation of the optical band gap energy.

F. Photo luminescence (PL)

Figure 5 shows that the synthesised NiO nanoparticles exhibit two prominent PL peaks at 413 nm and 433 nm, corresponding to electronic transitions associated with defects. The 413 nm peak (≈3.00 eV) is attributed to near-band-edge emission, providing evidence of semiconductor nature and crystallinity. The 433 nm peak (≈2.86 eV) is attributed to defects such as oxygen or nickel vacancies, surface defects, and interstitial oxygen created during the green synthesis, which provide local energy levels that enable radiative recombination. The wide emission band between 430 and 600 nm may be attributed to several surface and structural defect states, persisting on a nanostructured NiO surface with a large surface-to-volume ratio, and to phytochemicals from the Terminalia mantaly extract, which act as a reducing and capping agent. A moderate degree of PL intensity suggests that the rate of electron–hole recombination is slightly lower, which is favourable for the photocatalytic reaction, as more electron–hole pairs can generate reactive species such as OH and O_2 radicals, increasing efficiency. In general, the PL results reveal that the green-synthesised NiO sample possesses an appropriate defect concentration for charge separation and crystallinity, which are suitable for its applications in photocatalytic, antibiotic, and optoelectronic fields.

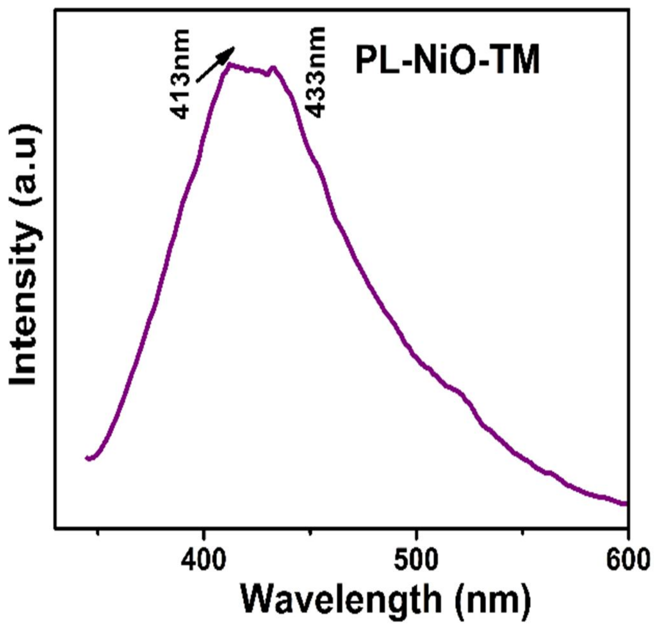

Figure 5. Photoluminescence (PL) spectrum of green synthesized NiO nanoparticles.

IV. APPLICATION

A. Antibacterial Activity Against Staphylococcus aureus and Enterococcus faecalis

The synthesised samples were tested for antibacterial activity against the Gram-positive bacterial strains Staphylococcus aureus and Enterococcus faecalis using the agar disc diffusion method. The images show the inhibition zones that formed around the test discs, indicating the susceptibility of the bacterial strains to the synthesised materials. In both images, the central disc (PC) was left unaltered, while the surrounding discs were test discs with varying levels of antibacterial activity.

The inhibition zones of (a) various concentrations of the sample against S. aureus were observed to be 0.0 mm, 3.2 mm, 4.3 mm, 6.1 mm, 7.4 mm and 9.6 mm. One concentration showed no effect (0 mm), while the others showed increasing zones with increasing concentration, suggesting that antibacterial activity increased with concentration. The maximum zone of inhibition was 9.6 mm. Irregular zones are indicative of natural diffusion and realistic assay conditions. Larger zones indicate enhanced interaction between nap and bacterial cell walls, leading to disruption of the cell walls, generation of ROS, denaturation of proteins, leakage of cell components, etc., which inhibit growth. Figure-b shows that for E. faecalis the Activity Zones increase with concentration, that is, 2.0 mm, 4.4 mm, 6.4 mm, 8.3 mm and 10.2 mm, which shows the best efficacy for this strain. However, the amount of E. faecalis present did not seem to affect the effectiveness of growth inhibition, as seen with higher levels of culture, which may be linked to higher levels of ROS, disruption of the membrane and interference with cellular processes.

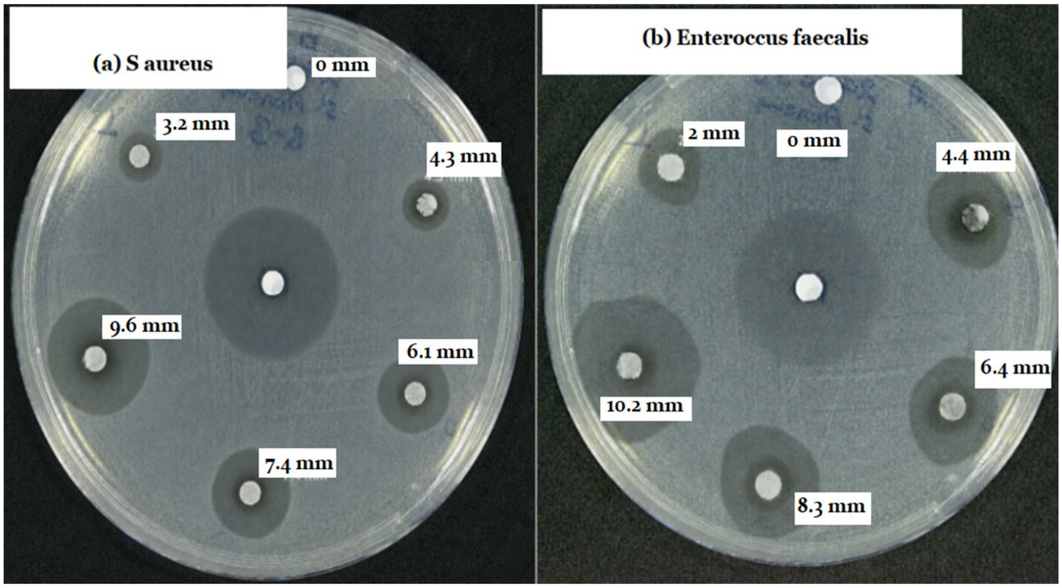

Figure 6. Antibacterial efficacy of green-synthesised NiO nanoparticles against (a) *Staphylococcus aureus* and (b) *Enterococcus faecalis* demonstrating concentration-dependent inhibition zones.

V. DISCUSSION AND CONCLUSIONS

Comparisons of the two bacterial strains show that the samples exhibited antibacterial activity against both Staphylococcus aureus and Enterococcus faecalis. However, the extent of inhibition varied with the concentration of the sample loaded. There was no difference between the maximum inhibition zones observed for E. faecalis (10.2 mm) and S. aureus (9.6 mm), indicating that E. faecalis was slightly more susceptible under the experimental conditions. Lower inhibition values (2.0-4.4 mm) indicate relatively weak antibacterial activity, while higher inhibition values (more than 6 mm) indicate relatively moderate antibacterial activity. Overall, the results support the conclusion that the synthesised nanoparticles exhibit concentration-dependent antibacterial activity against all Gram (+) bacterial strains tested and have the potential to be used as environmentally friendly antimicrobial agents.

Future scope

Large scale production of nickel oxide nanoparticles for industrial purposes can be an extension of this work.

Acknowledgements

The authors are thankful to Anurag University and Hyderabad Central University (HCU) for synthesising and characterisation techniques. One of the authors (BL) would like to thank the Head of the Department of Physics, Anurag University, Hyderabad, for his encouragement and support.

Conflict of Interest. None.

REFERENCES

[1] Anuradha . G, Lavanya.B and Ramana.M.V., Silver Nanoparticles From Terminalia mantaly : Biogenic synthesis and characterization (2025), Journal of Advances in Science, Engineering and Technology, 1,1, 46-53.

[2] Azam, A., Ahmed, F., Arshi, N., Chaman, M., & Naqvi, A. H. (2009). One step synthesis and characterization of gold nanoparticles and their antibacterial activities against E. coli (ATCC 25922 strain). IntIernational Journal of Theoretical and Applied Sciences, 1(2), 1–4.

[3] Balakrishnan, K., Thangavel, G., & Murugesan, N. (2023). Structural, morphological, optical and electrochemical. In Int. J. Nano Dimens (Vol. 14, Issue 2).

[4] Bandari Lavanya, Y. Aparna, Mallu Chenna Reddy, M.Venkata Ramana, (2026)Green-Synthesized ZnO nanoparticles from plant extracts:Characterization, photo catalytic activity, and antibacterial activity, Ionics, 32, 849–866.

[5] Barve, A. K., Gadegone, S. M. & Lanjewar, R. B. (2021). .Synthesis and Morphological Study of Nickel Oxide Nanoparticle. International Journal of Advanced Research in Science, Communication and Technology, 1–5.

[6] Berhe, M. G., & Gebreslassie, Y. T. (2023). Biomedical Applications of Biosynthesized Nickel Oxide Nanoparticles. In International Journal of Nanomedicine (Vol. 18, pp. 4229–4251). Dove Medical Press Ltd.

[7] Biswas, P., Anand, U., Saha, S. C., Kant, N., Mishra, T., Masih, H., Bar, A., Pandey, D. K., Jha, N. K., Majumder, M., Das, N., Gadekar, V. S., Shekhawat, M. S., Kumar, M., Radha, Proćków, J., Lastra, J. M. P. de la, & Dey, A. (2022). , "Betelvine (Piper betle L.): A comprehensive insight into its ethnopharmacology, phytoche. In Journal of Cellular and Molecular Medicine, 26(11), 3083–3119. John Wiley and Sons Inc.

[8] Chandra, H., Patel, D., Kumari, P., Jangwan, J. S., & Yadav, S. (2019). Phyto-mediated synthesis of zinc oxide nanoparticles of Berberis aristata: Characterization, antioxidant activity and antibacterial activity with special reference to urinary tract pathogens. Materials Science and Engineering C, 102, 212–220.

[9] Dejam, L., Sabbaghzadeh, J., Ghaderi, A., Solaymani, S., Matos, R. S., Tălu, Stefan, da Fonseca Filho, H. D., Sari, A. H., Kiani, H., Shayegan, A. H. S., & Doudaran, M. A. (2023). Advanced nano-texture, optical bandgap, and Urbach energy analysis of NiO/Si heterojunctions. Scientific Reports, 13(1).

[10] El-Kemary, M., Nagy, N., & El-Mehasseb, I. (2013). Nickel oxide nanoparticles: Synthesis and spectral studies of interactions with glucose. Materials Science in Semiconductor Processing, 16(6), 1747–1752.

[11] Ezhilarasi, A. A., Vijaya, J. J., Kaviyarasu, K., Zhang, X., &Kennedy, L. J. (2020). Green synthesis of nickel oxide nanoparticles using Solanum trilobatum extract for cytotoxicity, antibacterial and photocatalytic studies. Surfaces and Interfaces, 20.

[12] Hafeez, M., Shaheen, R., Akram, B., Ahmed, M. N., Zain-Ul-Abdin, Haq, S., Din, S. U., Zeb, M., & Khan, M. A. (2021). Green Synthesis of Nickel Oxide Nanoparticles using Populus ciliata Leaves Extract and their Potential Antibacterial Applications. South African Journal of Chemistry, 75.

[13] Hussain, S., Ali Muazzam, M., Ahmed, M., Ahmad, M., Mustafa, Z., Murtaza, S., Ali, J., Ibrar, M., Shahid, M., & Imran, M. (2023). Green synthesis of nickel oxide nanoparticles using Acacia nilotica leaf extracts and investigation of their electrochemical and biological properties. Journal of Taibah University for Science, 17(1).

[14] Iqbal, J., Abbasi, B. A., Mahmood, T., Hameed, S., Munir, A., & Kanwal, S. (2019). Green synthesis and characterizations of Nickel oxide nanoparticles using leaf extract of Rhamnus virgata and their potential biological applications. Applied Organometallic Chemistry, 33(8).

[15] Iravani, S., Korbekandi, H., Mirmohammadi, S. V. and Zolfaghari, B. (2014). Synthesis of silver nanoparticles: chemical, physical and biological methods. In Research in Pharmaceutical Sciences (Vol. 9)

[16] Jassim, S. M., Abd, M. A., & Hammed, I. A. (2023). Green synthesis of Nickel Oxide Nanoparticles using Syzygium Aromatic Extract: Characterization and Biological Applications. Al-Bahir Journal for Engineering and Pure Sciences, 2(2).

[17] Koparde, A., Shete, A., Patil, A., Mali, D., Durgawale, T., Yeligar, V. C., Shewale, M., Kadam, A. and Jadhav, R. (2023). Preparation and characterization of silver nanoparticles using Cissus quadrangularis extract and its in vitro anti-arthritic activity. Biological Forum-An International Journal, 15(3), 665-668.

[18] Mirzaei, H., & Darroudi, M. (2017). Zinc oxide nanoparticles: Biological synthesis and biomedical applications. Ceramics International, 43(1), 907–914.

[19] Lavanya.B, Aparna.Y and Ramana, M.V. (2025) Synthesis, characterization of zinc oxide nanoparticles using Terminalia mantaly leaf extract and their antibacterial activity, Materials Today Proceedings,19(2), 1011-1016.

[20] Lavanya.B, Aparna.Y and Venkata Ramana, M. (2024) Green Synthesis of Nickel Oxide Nanoparticles using Betel Leaf Extract and Oxalis stricta Leaf Extract and their Characterization, Biological forum- An International Journal, 16(7), 36-43

[21] Lavanya.B, Aparna.Y and Ramana, M.V. (2025), Iron Oxide Nanoparticles from Ocimum basilicum Leaf Extract: A Green route to Synthesis, characterization and Applications, Journal of Advances in Science, Engineering and Technology, 1,1,10-18

[22] Olajire, A. A., & Mohammed, A. A. (2020). Green synthesis of nickel oxide nanoparticles and studies of their photocatalytic activity in degradation of polyethylene films. Advanced Powder Technology, 31(1), 211–218.

[23] Praburaman, L., Jang, J. S., Muthusamy, G., Arumugam, S., Manoharan, K., Cho, K. M., Min, C., Kamala-Kannan, S., & Byung-Taek, O. (2016). Piper betle-mediated synthesis, characterization, antibacterial and rat splenocyte cytotoxic effects of copper oxide nanoparticles. Artificial Cells, Nanomedicine and Biotechnology, 44(6), 1400–1405.

[24] Rahdar, A., Aliahmad, M., & Azizi, Y. (2015). NiO Nanoparticles: Synthesis and Characterization. In JNS(Vol. 5).

[25] Ramesh, P., & Rajendran, A. (2022). Green synthesis of nickel oxide nanoparticles for photodegradation analysis. Materials Today: Proceedings, 68, 367–372.

[26] Sabouri, Z., Rangrazi, A., Amiri, M. S., Khatami, M., & Darroudi, M. (2021). Green synthesis of nickel oxide nanoparticles using Salvia hispanica L. (chia) seeds extract and studies of their photocatalytic activity and cytotoxicity effects. Bioprocess and Biosystems Engineering, 44(11), 2407–2415.

[27] Sagadevan, S., Fatimah, I., Anita Lett, J., Rahman, M. Z., Leonard, E., & Oh, W. C. (2023). Eco-friendly green approach of nickel oxide nanoparticles for biomedical applications. In Open Chemistry (Vol. 21, Issue 1). Walter de Gruyter GmbH.

[28] Selvanathan, V., Shahinuzzaman, M., Selvanathan, S., Sarkar, D. K., Algethami, N., Alkhammash, H. I., Anuar, F. H., Zainuddin, Z., Aminuzzaman, M., Abdullah, H., & Akhtaruzzaman, M. (2021). Phytochemical-assisted green synthesis of nickel oxide nanoparticles for application as electrocatalysts in oxygen evolution reaction. Catalysts, 11(12).

[29] Sharma, A. K., Desnavi, S., Dixit, C., Varshney, U., & Sharma, A. (2015). Extraction of Nickel Nanoparticles from Electroplating Waste and Their Application in Production of Bio-diesel from Biowaste. International Journal of Chemical Engineering and Applications, 6(3), 156–159. https://doi.org/10.7763/ijcea.2015.v6.472

[30] Tile, V. G., Suraj, H., Uday, B., & Sahana, S. (2016). Recent Trends in Nanotechnology and its Future Scope-A Review. International Journal on Emerging Technologies (Special Issue on ICRIET-2016), 7(2), 377–385.

[31] Uddin, S., Safdar, L. Bin, Anwar, S., Iqbal, J., Laila, S., Abbasi, B. A., Saif, M. S., Ali, M., Rehman, A., Basit, A., Wang, Y., & Quraishi, U. M. (2021). Green synthesis of nickel oxide nanoparticles from berberis balochistanica stem for investigating bioactivities. Molecules, 26(6).

[32] Veerasamy, R., Xin, T. Z., Gunasagaran, S., Xiang, T. F. W., Yang, E. F. C., Jeyakumar, N., & Dhanaraj, S. A. (2011). Biosynthesis of silver nanoparticles using mangosteen leaf extract and evaluation of their antimicrobial activities. Journal of Saudi Chemical Society, 15(2), 113–120.